Journal Name

COMMUNICATION

Structure-directing effects in (110)-layered hybrid perovskites containing two distinct organic moieties

Received 00th January 20xx,
Accepted 00th January 20xx

DOI: 10.1039/x0xx00000x

www.rsc.org/

Yuan-Yuan Guo[a], Jason A. McNulty[a], Natalie Mica[b], Ifor D. W. Samuel[b], Alexandra M. Z. Slawin[a], Michael Bühl[a] and Philip Lightfoot*[a]

The hybrid perovskites (ImH)(GuH)$PbBr_4$ and (TzH)(GuH)$PbBr_4$ (ImH^+ = imidazolium, GuH^+ = guanidinium, TzH^+ = 1,2,4-triazolium) both adopt (110)-oriented layer structures. However, the GuH^+ cation adopts differing crystallographic sites in the two structures (*intra*-layer versus *inter*-layer); this is discussed in terms of the sizes of the organic cations and their hydrogen-bonding preferences.

The exploratory synthesis of new hybrid halide perovskites has seen a huge upsurge of activity recently, due to the relevance of these materials to solar cell and luminescence applications.[1-3] Amongst the known families of layered perovskites, those based on so-called (001) orientation (i.e. the cubic perovskite parent structure is sliced across the octahedral apices) are by far the most common.

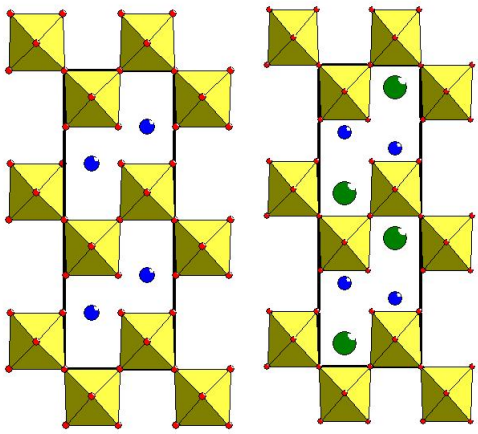

Fig. 1. Aristotype structures for (110)-oriented layered perovskites ABX4 (left) and AA´BX_4 (right)

An alternative structural family (the (110)-oriented layered perovskites; where the structure is sliced across an octahedral edge) occurs in a much more limited compositional space and evidently requires more stringent crystal-chemical criteria for its stability.

In fact, in purely inorganic compositions, there are two closely related families of (110)-oriented perovskites (Figure 1). These have generic compositions ABX_4 (X = oxide or fluoride)[4,5] and AA´BX_4 (X = oxide)[6] and can be represented by the aristotype (i.e. highest possible symmetry) compositions $BiReO_4$[7] and $NdBaScO_4$,[8] both of which crystallise in the orthorhombic space group *Cmcm*. Note that the A and A´ cations order fully in the $NdBaScO_4$ structure such that the larger Ba^{2+} occupies the 'intra-layer' site (A´), tucked within the perovskite-like A site (resulting in a coordination number of 11), whereas the smaller Nd^{3+} occupies the 'inter-layer' site (A), with a coordination number of seven.

Hybrid analogues of these structure types occur for the larger halides. Specifically, Smith *et al*.[1] record nine examples, *viz.* two Sn-I, one Pb-Cl, four Pb-Br and two Pb-I based compositions, but the number of examples continues to grow.[9,10] However, the vast majority of these phases correspond to the ABX_4 family (i.e. they contain A^{2+} diamines). The only previously known hybrid examples of the family AA´BX_4 are cases where A and A´ are the same (guanidinium) cation in $(GuH)_2SnI_4$[11] and $(GuH)_2PbI_4$[12] and two cases where A and A´ are different: $(H_2NC(I)NH_2((CH_3NH_3)MI_4$ (M = Sn[13] or Pb[14]).

In this paper we present two further examples of this unusual class of AA´BX_4 materials. Inspired by the two observations above: (i) GuH^+ acting alone templates this structure type, and (ii) a combination of two cations having distinct sizes and hydrogen bonding preferences leads to cation-ordered (110) structures, we chose to focus on mixed cation systems having 'disc-shaped' monoprotonated amines of similar sizes, *viz.* GuH^+, ImH^+ and TzH^+.

Details of synthesis and characterisation are provided in ESI. The crystal structures of (ImH)(GuH)$PbBr_4$ ("IGPbBr$_4$") and (TzH)(GuH)$PbBr_4$ ("TGPbBr$_4$") were determined by single crystal XRD at temperature of 298 K and 93 K. IGPbBr$_4$ adopts the same structure at each temperature, with the GuH^+ moiety exhibiting disorder over two positions around its pseudo 3-fold axis (see ESI for further

[a] School of Chemistry and EaStChem, University of St Andrews, St Andrews, Fife, KY16 9ST, U.K. E-mail: pl@st-andrews.ac.uk
[b] Organic Semiconductor Centre, SUPA, School of Physics, University of St Andrews, St Andrews, Fife, KY16 9SS, U.K. E-mail: pl@st-andrews.ac.uk

‡Electronic Supplementary Information (ESI) available: Synthesis, single crystal and powder XRD, distortion mode analysis, crystallographic data (CIF). CIF data have been deposited with CCDC: deposition numbers 1917733-1917736
See DOI: 10.1039/x0xx00000x

details). On the contrary, $TGPbBr_4$ exhibits disorder of the TzH^+ moiety at 298 K, and no disorder of the GuH^+. The disorder freezes out to a well-ordered structure at 93 K with a change of space group

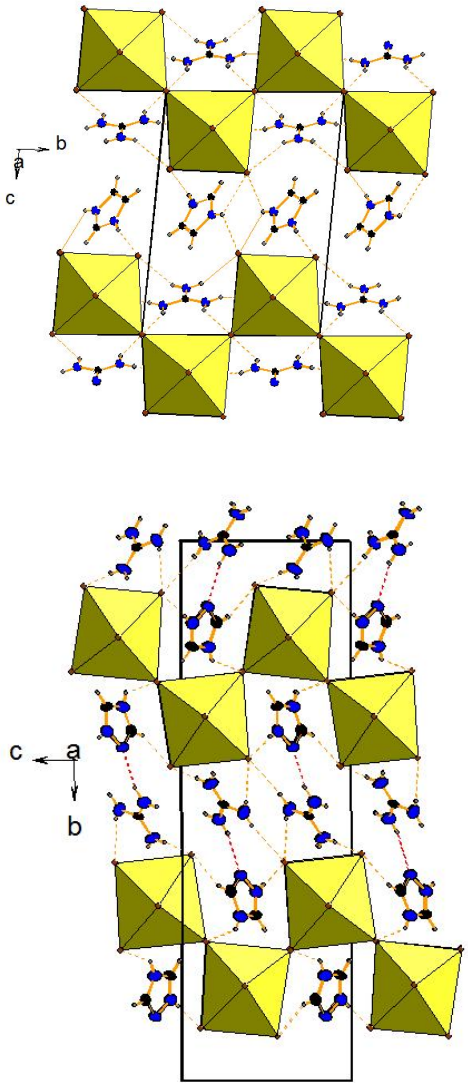

Fig. 2. Crystal structures at 93 K of (top) $IGPbBr_4$ and (below) $TGPbBr_4$. Note the octahedral tilting and the inter-cationic $GuH^+ \rightarrow TzH^+$ H-bond in $TGPbBr_4$.

from $P2/c$ to $P2_1/c$ and an effective doubling of the *b* axis, due to the ordering of the organic moieties and correlated octahedral tilting around the *a* axis. Figure 2 shows the crystal structures at 93 K; further details are provided in ESI. A further, immediately apparent feature of the structures is that GuH^+ occupies differing positions within each structure, *i.e*. the intra-layer (A´) site in $IGPbBr_4$ but the inter-layer (A) site in $TGPbBr_4$. Ionic size effects are the first factor that may influence this feature, but it is clear from the nature of the disorder that there may also be some frustration of intermolecular interactions, so hydrogen-bonding also needs to be carefully considered in understanding the subtle features of this structural behaviour.

In attempting to understand the differing cation ordering behaviour between the two compounds, we first consider ionic size effects. Kieslich *et al*.[15] used a simple 'spherical ion' model, based on rotation of the molecule around its centre of mass, to determine a consistent set of ionic radii for several small nitrogen-based cations, including ImH^+ and GuH^+. Unfortunately, TzH^+ was not included in that work. Since then, more sophisticated computational methods have been used to define molecular sizes for some of the organic cations. For example, Filip *et al*.[16] used DFT methods to estimate ionic size by taking into account a sphere which included 95% of the electron density. Becker *et al*.[17], used a DFT method also based on rotation around the molecular centre of mass: the radius of the sphere which contained the complete isocharge density was taken as the effective ionic radius. We have used two slightly different DFT-based methods to calculate ionic radii for the same set of molecular cations, but also include TzH^+ in our list. Further details of our methods are provided in ESI but, briefly: Method 1 involves calculating the molecular volume by integrating over the total electron densities, making no assumption about molecular shape. These volumes are then converted to effective radii for a sphere of the same volume. Method 2 involves encapsulating the molecular cation in a cuboctahedral array of Ne atoms and using the optimised Ne-Ne distances to calculate effective ionic radii.

Our values for ionic radii are provided in Table 1, and compared to those of Kieslich[15] and Becker.[17] As can be seen, the two quantum-mechanical approaches we use agree remarkably well with each other, but generally give lower estimations of effective radii than Becker's method, probably due to the fact that we do not assume spherical symmetry. Perhaps surprisingly, our own calculations are in closer agreement with the more empirical estimates of Kieslich. In both our approaches it is seen that TzH^+ is probably a few pm smaller than ImH^+, but of a similar size to GuH^+. The data of Becker support the assertion that ImH^+ is larger than GuH^+ whereas those of Kieslich contradict this. However, the differences are relatively small and unlikely in themselves to be the only driving force for the observed cation ordering in $IGPbBr_4$ and $TGPbBr_4$.

Another approach to using the radii might be to calculate perovskite-like tolerance factors, *t*, for a hypothetical "$APbBr_3$" cube to approximate the intra-layer site environment. These values are derived using the both the standard "Shannon" radii[18] for all ions and also using the modified (smaller) Pb^{2+} radius suggested by Travis.[19] The corresponding values for the oxide analogue $NdBaScO_4$ (using the Shannon radii) are also given in Table 2. The values for $NdBaScO_4$ rationalise why the 'larger' cation prefers the intra-layer (A´) site in the oxides allowing a 'snug fit' for Ba^{2+}. However, in the case of the hybrid bromides studied here, all *t* factors are well above the ideal value of 1. Obviously, there is more flexibility in this structure type than in a cubic perovskite, but the high tolerance factors for ImH^+ suggest that size may indeed be a critical factor in precluding its occupancy of the intra-layer site, and GuH^+ is preferred to occupy this site in $IGPbBr_4$.

For the GuH^+/TzH^+ pairing the size difference is less important, and hydrogen-bonding effects might be considered to play a decisive role in $TGPbBr_4$. A clue to this is seen in Figure 2, where the enhanced H-bonding options of the GuH^+/TzH^+ pair allow an inter-cation H-bond to the unprotonated nitrogen of the TzH^+ moiety, perhaps stabilising interactions between adjacent lead bromide layers. A further feature

here is that occupancy of the intra-layer site by TzH^+ rather than GuH^+ apparently allows octahedral tilting to occur in the lead bromide layers, at least at lower temperatures, further optimising intermolecular interactions. On the contrary, the retention of disorder of the GuH^+ moiety in $IGPbBr_4$, even at lower temperatures, coupled with no octahedral tilting, suggests that no satisfactory additional intermolecular interactions can be formed in this case.

Table 1. Comparison of molecular ionic radii based on the methods introduced here[i], versus those of Kieslich[15] and Becker[17]

Cation[ii]	Radius (pm)			
	Method 1	**Method 2**	**Kieslich**	**Becker**
NH_4^+	194	177	146	170
MAH^+	235	227	217	238
FAH^+	247	245	253	277
HAH^+	226	213	217	220
AZH^+	276	272	250	284
HYH^+	217	202	216	226
EAH^+	265	262	274	299
DMH^+	265	263	272	296
TMH^+	309	307	292	301
ImH^+	274	273	258	303
GuH^+	266	272	278	280
TzH^+	268	269		

i. Methods 1 and 2 are based on simple molecular volumes and optimisations in a cuboctahedral array of Ne atoms, respectively (B3LYP-D3/6-31+G** level, see ESI).
ii. MaH^+ = methylammonium; FAH^+ = formamidinium; HAH^+ = hydrazinium; AZH^+ = azetidinium; HYH^+ = hydroxylammonium; EAH^+ = ethylammonium; DMH^+ = dimethylammonium; TMH^+ = tetramethylammonium.

Table 2. Tolerance factors (t)[i] for selected compositions adopting the (110) perovskite structure

Composition	Species in A´ site	t
$NdBaScO_4$	Ba	0.99
$NdBaScO_4$	Nd	0.88
$IGPbBr_4$	ImH^+	1.06; 1.20[ii]
$IGPbBr_4$	GuH^+	1.04; 1.15[ii]
$TGPbBr_4$	TzH^+	1.04
$H_2NC(I)NH_2((CH_3NH_3)SnI_4$	MAH^+	1.02; 1.02[iii]
$H_2NC(I)NH_2((CH_3NH_3)PbI_4$	MAH^+	1.01; 1.02

i. For a "cubic" perovskite ABX_3, $t = (r(A)+r(X))/\sqrt{2}(r(B)+r(X))$.
ii.The two values refer to calculations using different combinations of Pb^{2+} radius and molecular radii (Table 1): the first value is Shannon/Method 1 and the second is Travis/Becker. These represent the smallest and largest values of t for each ions pair.
iii.Travis radius for Sn^{2+} in each case.

It is worth noting that even the smaller molecular cations (*e.g.* methylammonium) result in $t > 1$ when using the Travis radii, which appears to justify the previously reported $(H_2NC(I)NH_2((CH_3NH_3)MI_4$ (M = Sn[13] or Pb[14]) adopting the (110) structure type. On the contrary, the largest monoatomic inorganic cation, Cs^+ (r = 188 pm), may be too small to stabilize the (110) structure in lead halides, with t factors significantly less than 1 by any of the calculation methods considered here. Indeed, $Cs(GuH)PbX_4$ (X = Br or I) has been shown to adopt the (001)-oriented layered structure.[20]

UV-vis absorbance spectra and photoluminescence (PL) measurements were carried out for both powder $IGPbBr_4$ and $TGPbBr_4$ and the spectra shown in Figure 3. The absorption spectra of both compositions feature similar peaks at ~370 nm (3.4 eV) and ~395 nm (3.1 eV). Band gaps (as derived from the Tauc plot; see ESI) are 2.94 eV for $IGPbBr_4$ and 2.88 eV for $TGPbBr_4$. Interestingly, the emission spectra appear drastically different for the two compounds. A strong narrow peak is observed at 563 nm (FWHM = 20 nm) in $IGPbBr_4$ when excited at 370 nm. In contrast, a broad peak is observed at 701 nm (FWHM = 130 nm) in $TGPbBr_4$ when excited at the same wavelength.

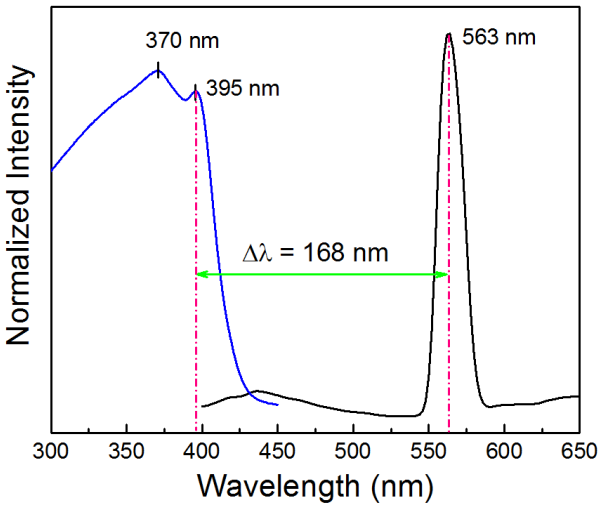

(a)

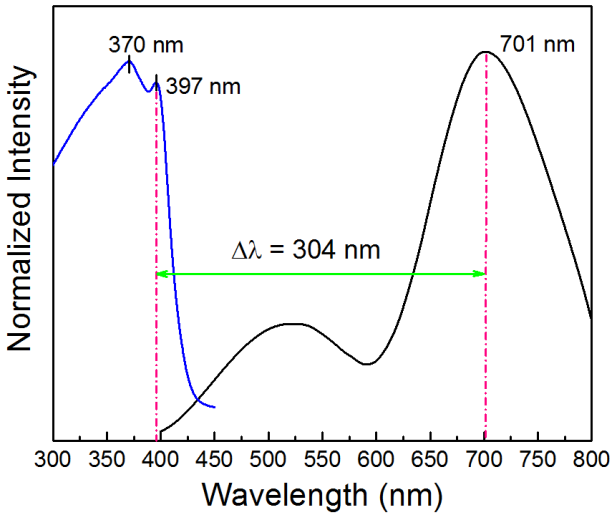

(b)

Fig. 3. Absorption and emission spectra (excited at 370 nm) for (a) $IGPbBr_4$ and (b) $TGPbBr_4$.

Previous work regarding (110)-oriented 2D halide perovskites associated the broad PL emission with high levels of structural

distortions[9]. The mean distortion level and the bond angle variance of each octahedron in both compositions were calculated (details are provided in ESI) and the calculated values indicate that the $PbBr_6$ octahedra in the $TGPbBr_4$ ($\Delta d = 10.97\times10^{-4}$ and $\sigma^2 = 28.22$) structure are significantly more distorted than in $IGPbBr_4$ ($\Delta d = 7.39\times10^{-4}$ and $\sigma^2 = 16.16$). This is consistent with the observation of a broad emission spectrum in $TGPbBr_4$ but not in $IGPbBr_4$.

Sharp, narrow luminescence has previously been reported to be attributable to radiative recombination of free excitons[21]. While this has not been investigated in this study, variable temperature PL measurements could be utilised due to the temperature dependence of this response. In $IGPbBr_4$ this is hypothesised to result in the gradual loss of the sharp intense peak and the subsequent observation of a broad feature similar to that observed in $TGPbBr_4$.

In summary, we have prepared two new examples of a rare structural type amongst lead halide perovskites, viz. the (110)-oriented $AA'BX_4$ structure. Ordering of the organic cations guanidinium, imidazolium and 1,2,4-triazolium across the intra-layer and inter-layer sites is observed, and this is discussed in terms of ionic size effects and hydrogen-bonding factors. The discussion here suggests that both ionic size effects and specific H-bonding opportunities/preferences influence the adoption of the (110)-oriented perovskite structure in the $AA'BX_4$ family. However, we can provide no definitive structural prediction formula based on the data available so far. The competing factors are complex, as shown by the preference of GuH^+ for two different sites in the examples here. Moreover, both G_2SnI_4 (t = 1.12 based on the Travis/Becker radii) and G_2PbI_4 (t = 1.09 based on the Travis/Becker radii) adopt this structure type[11], but both display a series of phase transitions as a function of temperature, involving re-orientation of GuH^+. On the contrary, G_2PbBr_4 (t = 1.14) adopts a very different structure type containing $PbBr_5$ polyhedra in edge-shared chains.[20] These observations perhaps imply that GuH^+ can be accommodated in a variety of local structural arrangements, perhaps related to its choice of H-bonding opportunities, with six potential H-bond donors.

We also introduce two DFT-derived sets of radii for common organic cations, which do not involve spherical averaging, and which may therefore be more appropriate for non-cubic perovskites, such as the layered hybrid ones studied here. Preliminary luminescence measurements are presented which suggest a quite different nature of light emission from the two new compounds.

This study prompts further work to probe the composition dependence of this interesting structure type, in order to map out its stability limits in terms of the relative sizes and hydrogen-bonding effects of the constituent organic species. More detailed correlations of structure, composition and photophysical properties should then be carried out.

We acknowledge support from the University of St Andrews, the China Scholarship Council (studentship to YYG) and the Leverhulme trust (RPG-2018-065). Calculations were performed on a local computer cluster maintained by Dr H. Früchtl. There are no conflicts of interest to declare.

The research data supporting this publication can be accessed at xxxxxx

Notes and references

1 M. D. Smith, E. J. Crace, A. Jaffe, and H. I. Karunadasa, *Annu. Rev. Mater. Res.,* 2018, **48**, 111-136.
2 C. Katan, N. Mercier and J. Even, *Chem. Rev.*, 2019, **119**, 3140-3192.
3 L. Mao, C. C. Stoumpos and M. G. Kanatzidis, *J. Am. Chem. Soc.*, 2019, **141**, 1171-1190.
4 K. J. Cordrey. M. Stanczyk, C. A. L. Dixon, K. S. Knight, J. Gardner, F. D. Morrison and P. Lightfoot, *Dalton Trans.*, 2015, **44**, 10673-10680.
5 S. W. Kim, H. Y. Chang and P. S. Halasyamani, *J. Am. Chem. Soc.*, 2010, **132**, 17684-17685.
6 K. Fujii, Y. Esaki, K. Omoto, N. Yashima, A. Hoshikawa, T. Ishigaki and J. R. Hester, *Chem. Mater.*, 2014, **26**, 2488-2491.
7 A. R. Rae Smith and A. K. Cheetham, *J. Solid State Chem.*, 1979, **30**, 345-352.
8 A. K. Cochrane, M. Telfer, C. A. L. Dixon, W. Zhang, P. S. Halasyamani, E. Bousquet and P. Lightfoot, *Chem. Commun.*, 2016, **52**, 10980-10983.
9 X. Li, P. Guo, M. Kepenekian, I. Hadar, C. Katan, J. Even, C. C. Stoumpos, R. D. Schaller and M. G. Kanatzidis, *Chem. Mater.*, 2019, **31**, 3582-3590.
10 R. Gautier, F. Massuyeau, G. Galnon and M. Paris, *Adv. Mater.*, 2019, **31**, 1807383.
11 M. Daub, C. Haber and H. Hillebrecht, *Eur. J. Inorg. Chem.*, 2017, 1120-1126.
12 M. Szafranski and A. Katrusiak, *Phys. Rev. B*, 2000, **61**, 1026-1035.
13 D. B. Mitzi, S. Wang, C. A. Field, C. A. Chess and A. M. Guloy, *Science*, 1995, **267**, 1473-1476.
14 Q. Wang, C. Jiang, P. Zhang and T. W. Hamann, *J. Phys. Chem. C*, 2018, **122**, 14177-14185.
15 G. Kieslich, S. Sun and A. K. Cheetham, *Chem. Sci.*, 2014, **12**, 4712-4715.
16 M. R. Filip, G. E. Eperon, H. J. Snaith and F. Giustino, *Nat. Commun.*, 2014, **5**, 5757.
17 M. Becker, T. Kluner and M. Wark, *Dalton Trans.*, 2017, **46**, 3500-3509.
18 R. D. Shannon, *Acta Cryst.*, 1976, **A32**, 751-767.
19 W. Travis, E. N. K. Glover, H. Bronstein, D. O. Scanlon and R. G. Palgrave, *Chem. Sci.*, 2016, **7**, 4548-4556.
20 O. Nazarenko, M. R. Kotyrba, M. Worle, E. Cuervo-Reyes, S. Yakunin and M. V. Kovalenko, *Inorg. Chem.*, 2017, **56**, 11552-11564.
21 M. D. Smith, B. L. Watson, R. H. Dauskardt and H. I. Karunasada, *Chem. Mater.*, 2017,**29**, 7083-7087.

